Am J Transl Res 2017;9(8):3586-3598
www.ajtr.org /ISSN:1943-8141/AJTR0046366

Original Article

MicroRNA-130a-3p suppresses cell viability, proliferation and invasion in nasopharyngeal carcinoma by inhibiting *CXCL12*

Rongfeng Qu, Yan Sun, Yarong Li, Chunmei Hu, Guang Shi, Yan Tang, Dongrui Guo

Department of Hematology and Oncology, The Second Hospital of Jilin University, Changchun 130041, Jilin, China

Received December 11, 2016; Accepted July 7, 2017; Epub August 15, 2017; Published August 30, 2017

Abstract: Incidence of nasopharyngeal carcinoma (NPC) has remained high worldwide, posing a serious health problem. MicroRNAs (miRNAs) are a family of about 20-23 nucleotides small non-coding molecules, which play a significant role in NPC. In this study, we explored the molecular mechanisms of miR-130a-3p in inhibiting viability, proliferation, migration and invasion of NPC cells by suppressing *CXCL12*. The relative expression of miR-130a-3p and *CXCL12* mRNA expression in tissues and cells was measured by qRT-PCR. NPC cell line CNE-2Z was transfected with miR-130a-3p mimics, *CXCL12* siRNA, cDNA-*CXCL12* and negative control. Western Blot was performed to detect *CXCL12* expression. The MTT assay was performed to study cell viability. The colony formation assay was done to test cell growth. Flow cytometry was conducted to analyze cell cycle and apoptosis. The Transwell assay was used to investigate cell migration and invasion. The results found that the up-regulation of miR-130a-3p or down-regulation of *CXCL12* could inhibit viability, proliferation, migration and invasion of CNE-2Z cells. Luciferase-reporting system assay was performed to investigate miR-130a-3p could bind to the 3'UTR region of *CXCL12* and the overexpression of miR-130a-3p could suppress *CXCL12* expression. Collectively, our finding suggested demonstrated that miR-130a-3p could prohibit the progression of NPC by suppressing *CXCL12*, which might serve as potential therapeutic targets for NPC.

Keywords: Nasopharyngeal carcinoma, miR-130a-3p, *CXCL12*, proliferation, migration, invasion

Introduction

Nasopharyngeal carcinoma (NPC) was a head and neck cancer which particularly prevalent in China and Southeast Asia, and its estimated incidence was high between 20/100,000 and 50/100,000 per year [1]. Radiotherapy has been considered as the primary treatment for newly developed NPC. After treatment with intensity-modulated radiotherapy, the 5-year local relapse-free survival of early-stage NPC was over 90% [2]. However, the prognosis for advanced NPC was unpleasant with a 5-year survival rate ranging from 50% to 70%, which was primarily due to the radio-resistance of NPC and high metastasis to distant organs [3, 4]. Unfortunately, as high as 80-90% of NPC patients were confirmed with NPC until the advanced stage, since the anatomical sites and the early symptoms of NPC were not obvious [1]. Therefore, profound researches into the molecular regulation tumorigenesis and progression of NPC may provide new sight for novel therapeutic treatment for NPC.

MicroRNAs (miRNAs) were small functional non-coding RNAs with conserved sequences. By binding to the 3'-untranslated region (3'UTR) of corresponding mRNAs, miRNAs could inhibit gene expression, and thus modulate various critical cellular processes, including cell differentiation, cell proliferation, cell migration, and cell apoptosis [5]. Ectopic expression of miRNAs can act as either tumor suppressors or oncogenes by abnormally regulating gene expression [6], and the potential of miRNA profiling in cancer diagnosis was highlighted [7, 8]. Besides, multiple miRNAs have been identified to suppress the growth, proliferation, invasion and metastasis of NPC cells, such as miR-34b, miR-156a and miR-506 [9-11].

In previous studies, down-regulation of miR-130a-3p was found within ovarian cancer cells

[12], non-small cell lung cancer cells [13] and prostate cancer cells [14]. Consistently, a recent study has confirmed that the overexpression of miR-130a-3p could suppress the differentiation, proliferation, migration and invasion of hepatocellular carcinoma cells [15]. Nevertheless, there has been little evidence supporting that miR-130a-3p can retard the growth of NPC, and the molecular mechanism remains unsearchable. Hence, further investigation into miR-130a-3p was necessary, and the identification of the target gene of miRNA-130a-3p was critical.

C-X-C motif chemokine ligand 12 (*CXCL12*), also known as stromal cell-derived factor-1 or pre-B-cell-growth stimulating factor, has been predicted as the target of miR-130-3p. *CXCL12* belonged to the CXC chemokine family, and was overexpressed in various tumors, such as prostate cancer, breast cancer and ovarian cancer [16-18]. Within these tumors, by binding to its receptor CXCR4, *CXCL12* could lead to activation of the Src, PI3K/Akt, ERK and JNK pathways, so as to facilitate cellular migration and invasion [19].

In our study, we creatively investigated the role of miR-130a-3p in NPC carcinogenesis and progression by suppressing CXCL10, which might help us better understand the mechanism of miR-130a-3p in NPC and provide some evidences for developing new treatment targets for NPC.

Methods and materials

Clinical samples

Forty-three normal nasopharyngeal epithelial tissues and 35 NPC tissues were collected from the Second Hospital of Jilin University. AllNPC biopsy samples were obtained before patients receiving chemotherapy or radiotherapy. All the protocols in this study were approved by the Ethics Committee of the Second Hospital of Jilin University. All the patients have signed the consent form.

Cell culture

We chose human NPC cell lines CNE-2Z, HONE-1, C666-1 and normal nasopharyngeal epithelial cell line NP69 (BeNaCulture Collection, Suzhou, China). Cells were cultured in 90% Roswell Park Memorial Institute (RPMI)-1640 supplemented with 10% (2% for NP69 cells) fetal bovine serum (FBS) at 37°C in 5% CO_2.

Transfection

Cells were seeded in 6-well plates 1 day before transfection. When cells confluence reached 70%-80%, transfection was conducted using Lipofectamine™2000 (Invitrogen). The medium was replaced 4 h after transfection and the cells were incubated in a cell incubator. CNE-2Z cells were transfected with miR-130a-3p mimics or control oligonucleotides (Ribobio, Guangzhou, China). *CXCL12* siRNA (20 nmol) was transfected to CNE-2Z to knock down *CXCL12*. pcDNA3.1-*CXCL12* (1 ng) was transfected to CNE-2Z to overexpress *CXCL12* protein. pcDNA3.1 empty plasmid was as negative control (pcDNA3.1-NC), and miR-130a-3p mimics+pcDNA3.1-*CXCL12* (miR-mimics+pcDNA3.1-*CXCL12*) was as test group. The pcDNA3.1-*CXCL12* was purchased from GenePharma, China. The cells were harvested 48 h and 72 h after transfection.

Dual-luciferase reporter gene assay

The pGL4.13-*CXCL12* 3'UTR (wt-3'UTR) and pGL4.13-*CXCL12* 3'UTR-mut (mut-3'UTR) plasmids were constructed using pGL4.13 vector (Promega, Madison, WI, USA). For luciferase assay, CNE-2Z cells were transfected with wt-3'UTR or mut-3'UTR vectors by Lipofectamine™ 2000. About 48 h after transfection, the luciferase activities were measured with the Dual-Luciferase Reporter System. Four different transfected groups were analyzed as follows: wt-3'UTR+NC group, wt-3'UTR+miR-130a-3p mimics group, mut-3'UTR+NC group and mut-3'UTR+miR-130a-3p mimics group.

qRT-PCR

The total RNA was collected using TRIzol reagent (Invitrogen, Carlsbad, CA, USA) and reverse transcription was performed to obtain cDNA through a RT kit (Fermentas, Maryland, USA). Then the miRNA or mRNA expression levels were analyzed according to the manufacturers' protocols. The U6 or GAPDH were used as the endogenous control of miRNA and mRNA, respectively. Finally, the RNA relative expression levels were calculated with $2^{-\Delta\Delta Ct}$ method. The primer sequences for PCR were given in **Table 1**.

Table 1. The primers for conduction of qRT-PCR

	Forward primers	Reverse primers
GAPDH	5'-AACGGATTTGGTCGTATTG-3'	5'-GGAAGATGGTGATGGGATT-3'
U6	5'-CTCGCTTCGGCAGCACA-3'	5'-AACGCTTCACGAATTTGCGT-3'
miR-130a-3p	5'-GGCAGTGCAATGTTAAAAG-3'	5'-CAGTGCGTGTCGTGGAGT-3'
CXCL12	5'-GCCATGAACGCCAAGGTC-3'	5'-CGAGTGGGTCTAGCGGAAAG-3'

Western blot

Total proteins were extracted by RIPA lysis buffer and protein concentrations was measured using bicinchoninic acid (BCA) assay. About 30 μg proteins were separated by 10% SDS-PAGE electrophoresis. The proteins were then transferred to the polyvinylidenefluoride (PVDF) membrane. The membranes were blocked by 5% skimmed-milk in TBST buffer for 1 h, then incubated with rabbit-anti-human *CXCL12* polyclonal antibody (1:1000, Abcam, Cambridge, MA, USA) or with mouse-anti-human *β*-actin monoclonal antibody (1:10000, Abcam) overnight at 4°C. The membranes were washed with TBST for 3 times and incubated with horseradish peroxidase conjugated with anti-rabbit or anti-mouse secondary antibody (Abcam) for 1 h at room temperature. The film was developed and fixed using ECL solution.

MTT assay

CNE-2Z cells at logarithmic growth phase were seeded into 96-well plates at a density of 1000 cells per well, and each group had 7 duplicates. We analyzed cell viability at different time points (24 h, 48 h, 72 h and 96 h after seeding). Briefly, 20 μl MTT solution (5 mg/ml) was added to each well, then the cells were incubated at a cell incubator for another 4 h. Then 150 μl DMSO was added and finally the absorbance was acquired at 570 nm using a spectrophotometer. The average optical density (OD) was plotted against the time series.

Colony formation assay

CNE-2Z cells were seeded into 6-well plates at a density of 2000 cells per well. After incubation for 24 h, the non-adherent cells were removed, and the remaining cells continued to be cultured for 1 week. The colonies were fixed with 4% paraformaldehyde, stained with 1% crystal violet and countered under a microscope. Each colony should contain no less than 50 cells.

Cell apoptosis analysis

The transfected CNE-2Z cells were digested by 0.25% trypsin to get single cell suspension, and were centrifuged at 1000 rpm to collect cells. After being resuspended with 500 μl binding buffer, they were transferred to 5 ml flow tubes. Then they were stained with Annexin V plus PI or each alone for 10-20 min at room temperature. The data were acquired on a flow cytometer.

Transwell assay

CNE-2Z cells were firstly starved using serum-free media for 24 h, and were then digested with 0.25% trypsin. Then 500 μl cell suspension containing 50000 cells were added to the upper chambers coated with Matrigelgel, and 600 μl complete media were added to the lower chambers. The cells were incubated for 12 h, and then were fixed with 4% paraformaldehyde for 20 min. Later, they were stained with 1% crystal violet for 10 min. The cells that crossed the Matrigel gel membrane were counted under a microscope.

Scratch-wound healing assay

CNE-2Z cell monolayers were wounded by scratching the surface on the 6-well plate as uniformly as possible with a pipette tip. The scratched wells were washed several times with PBS to remove detached debris after scratching. Then RPMI 1640 containing lipofectamine reagent and siRNA (20 nM) and pcDNA3.1 plasmids (1 μg) were added to the scratched wells. The cells were then incubated for 24 h at 37°C. The initial wounding and the movement of the cells in the scratched area were photographically monitored and imaged using an Olympus CKX41 inverted microscope coupled with a digital imaging system at 0 h, 24 h.

Statistical analysis

The numerical data were presented as mean ± SD. Two-tailed Student's *t*-tests were used to analyze the differences between two groups. One-way analysis of variance (ANOVA) was performed for analysis of multiple groups. $P<0.05$ was considered statistically significant. All sta-

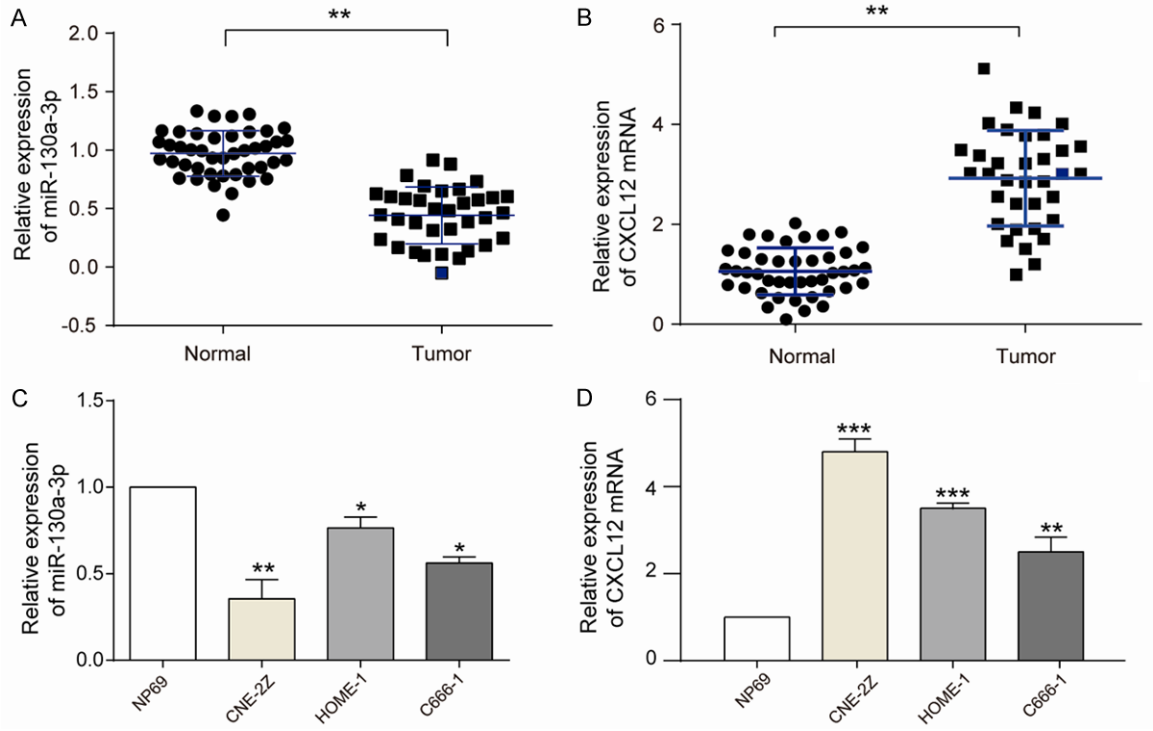

Figure 1. MiR-130a-3p and *CXCL12* expression in NPC tissues and cell lines. A, B: miR-130a-3p and *CXCL12* expression in 43 normal samples and 35 NPC samples, respectively, assessed by RT-qPCR. MiR-130a-3p expression is high in normal and low in NPC, whereas *CXCL12* expression is high in NPC and low in normal (student *t*-test, **P*<0.05, ***P*<0.01). C, D: qRT-PCR results showed that miR-130a-3p was significantly decreased in NPC cell lines (CNE-2Z, HONE-1, C666-1) when compared with normal nasopharyngeal epithelial cell line NP69. Adverse results appeared on *CXCL12* which was significantly increased in NPC cell lines (CNE-2Z, HONE-1, C666-1) when compared with NP69 (student *t*-test, ***P*<0.01, ****P*<0.001). The biggest expression disparity was found in CNE-2Z cell group. Each assay was conducted in triplicate and repeated three times. The data show the mean of triplicate repeats ± s.e.m.

tistical analyses were performed using SPSS 21.0 software (SPSS, Chicago, IL, USA).

Results

Down-regulated miR-130a-3p and up-regulated CXCL12 in NPC

The expression level of miR-130a-3p was significantly lower in NPC tissues than normal nasopharyngeal epithelial tissues (**Figure 1A**), whereas the expression of *CXCL12* showed the opposite results (**Figure 1B**). We also found the similar outcome appeared in 3 different NPC cell lines (CNE-2Z, HONE-1, C666-1), which had down-regulated miR-130a-3p expression (**Figure 1C**) and up-regulated *CXCL12* expression (**Figure 1D**) compared with the normal nasopharyngeal epithelial cell line (NP96). CNE-2Z cell line had the lowest miR-130a-3p and the highest *CXCL12* expression, which was chose for the following researches.

Overexpression of miR-130a-3p suppresses CNE-2Z cell viability, proliferation, migration and invasion

The RT-qPCR results showed that miR-130a-3p expression was higher in miR-130a-3p mimics group than control (empty) and NC (negative control) groups (**Figure 2A**) (*P*<0.01). The MTT assay results suggested that the relative cell viability of cells in miR-mimics group was much less active than other two groups (**Figure 2B**). The colony formation assay results showed that the CNE-2Z cells proliferation rate substantially dropped in miR-130a-3p mimics group (**Figure 2C**). Scratch-wound healing assay manifest that overexpressed miR-130a-3p had a lower migratory vitality (**Figure 2D**). Transwell assay was performed to analyze the cell invasion (**Figure 2E**). The result showed that the invasive ability of miR-130a-3p mimics group (60.2± 5.8%) was much weaker than other two groups.

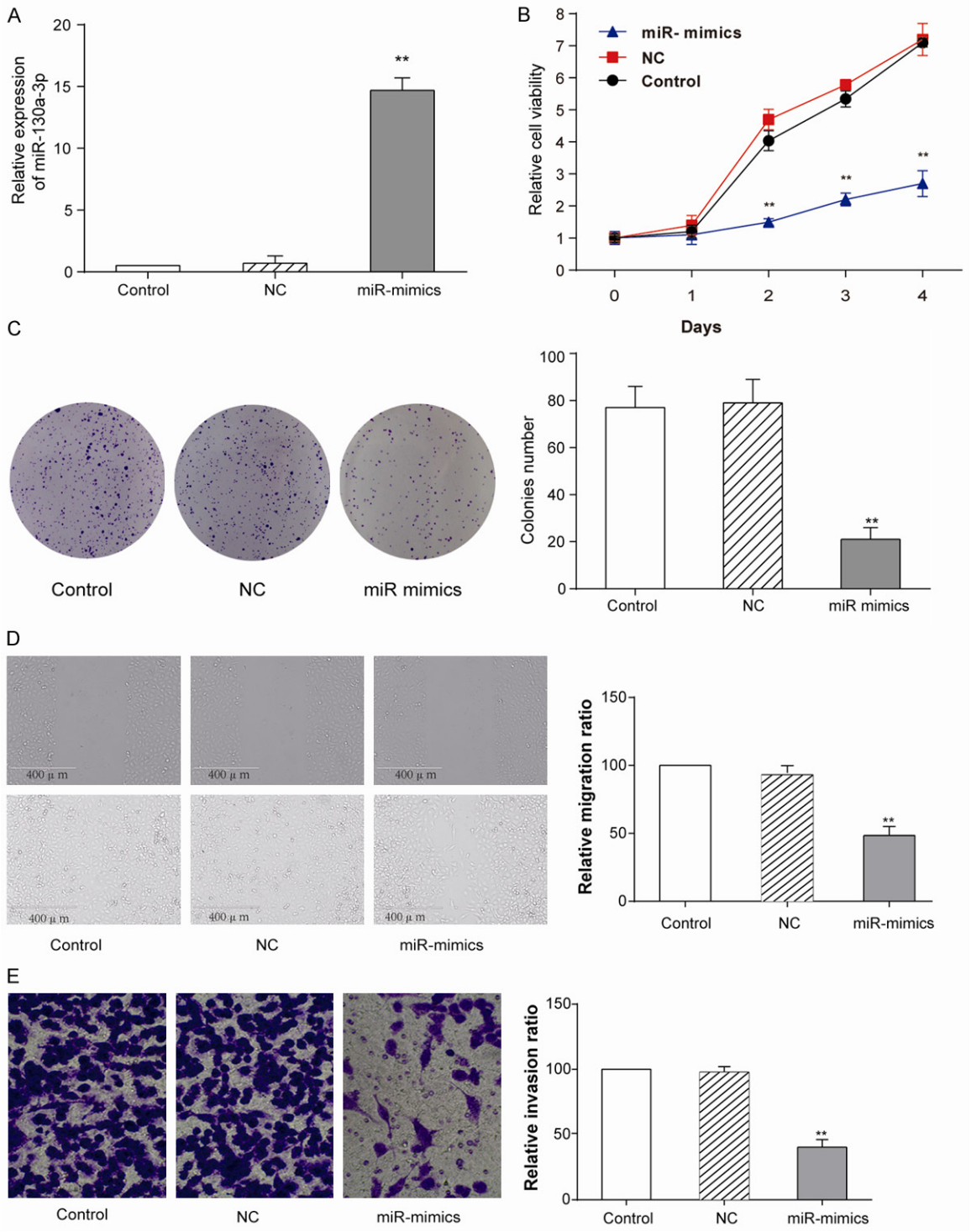

Figure 2. Overexpression of miR-130a-3p prohibited CNE-2Z cells. A: qRT-PCR experiments showed that miR-130a-3p was successfully transfected into CNE-2Z cells (student *t*-test, $^{**}P<0.01$). Control means empty transfection and NC as a transfected control. B: MTT assay was performed to analyze CNE-2Z cell viability at different time points (1-4 days), miR-130a-3p transfected group had a comparatively low cell viability (student *t*-test, $^{**}P<0.01$). C: Colony formation assay was also done to measure CNE-2Z cell proliferation rate. The advent of miR-mimics group was lower than control (student *t*-test, $^{**}P<0.01$). D: Scratch-wound healing assay was applied to analyze cell migration ability. Migration ability in miR-mimics group is lower than control (student *t*-test, $^{**}P<0.01$). E: Transwell assay was performed to analyze cell invasion ability. Invasion ability in miR-mimics group is lower (student *t*-test, $^{**}P<0.01$). Each assay was conducted in triplicate and repeated three times. The data show the mean of triplicate repeats ± s.e.m.

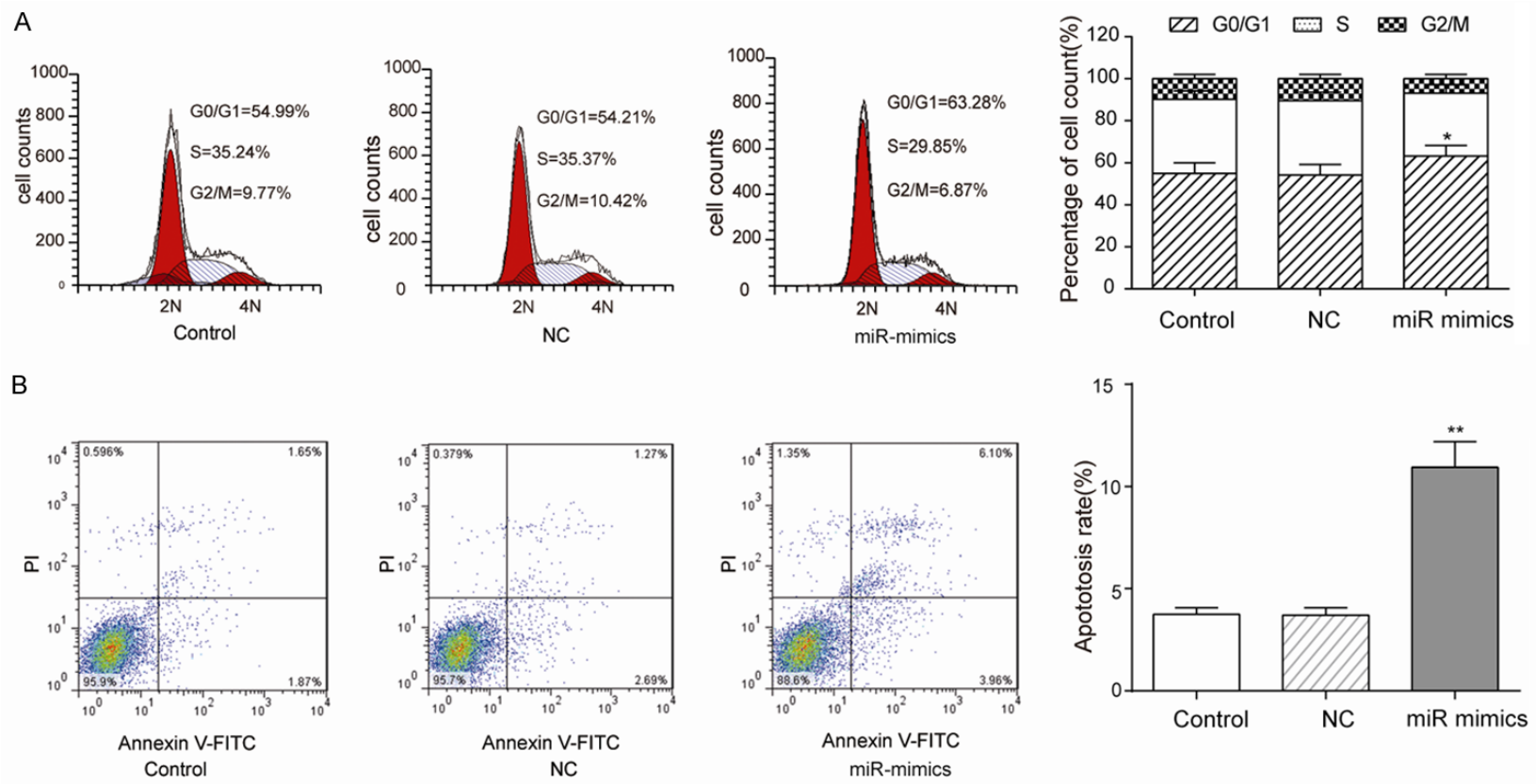

Figure 3. Overexpression of miR-130a-3p arresting CNE-2Z cells at G0/G1 stage and promoted apoptosis. A: CNE-2Z cell cycle was analyzed by flow cytometer (PI staining) 48 h post transfection. In the group of miR-mimics (overexpressed miR-130a-3p), the proportion of cells at G0/G1 stage was much higher than control and NC groups (student *t*-test, **P*<0.05). B: Annexin V and PI staining detected CNE-2Z cells apoptosis and miR-mimics group had higher ratio (student *t*-test, ***P*<0.01). Each assay was conducted in triplicate and repeated three times. The data show the mean of triplicate repeats ± s.e.m.

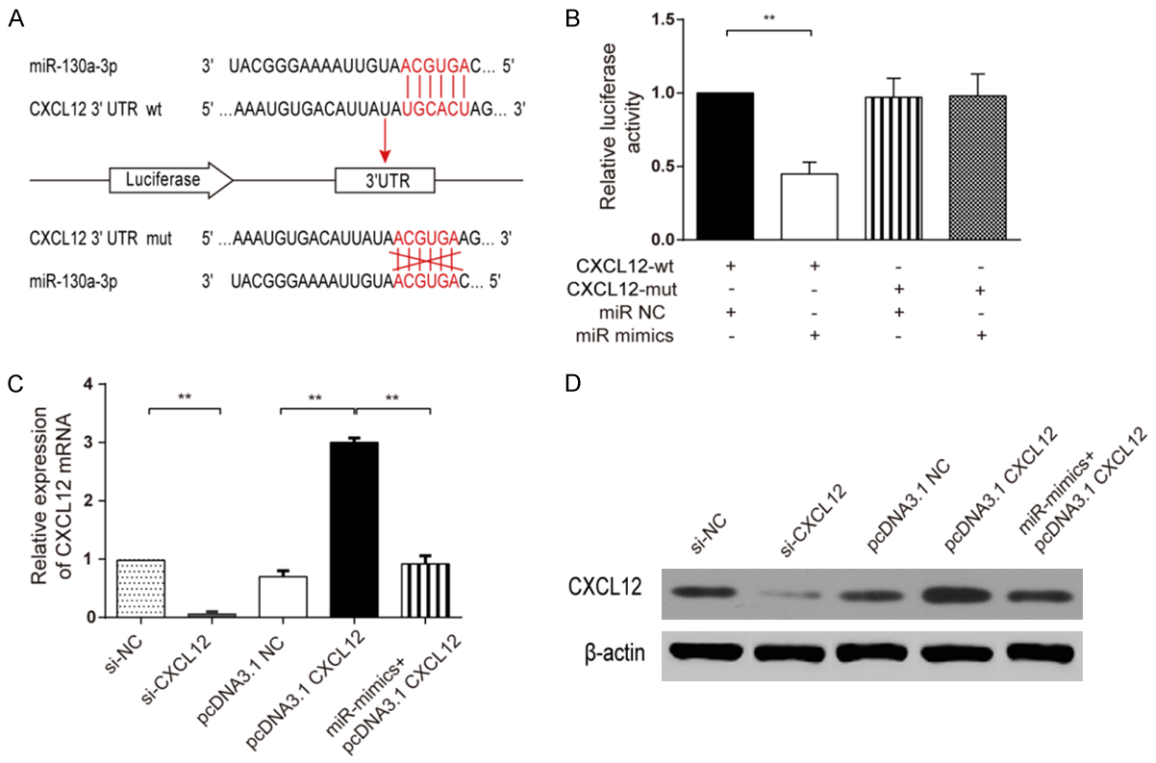

Figure 4. MiR-130a-3p inhibiting *CXCL12* expression. (A) Binding sites between miR-130a-3p and *CXCL12* 3'UTR and 6 mutant sites in *CXCL12* 3'UTR-mut would not complementary pairing to miR-130a-3p which be used as control. (B) Dual-luciferase assay showed that wt-3'UTR+miR-130a-3p mimics had a remarkably lower luciferase activity when compared with other three groups (student *t*-test, $**P<0.01$). (C) qRT-PCR and (D) Western Blot demonstrated that *CXCL12* level was remarkably decreased when miR-130a-3p was overexpressed (student *t*-test, $**P<0.01$). Each assay was conducted in triplicate and repeated three times. The data show the mean of triplicate repeats ± s.e.m.

MiR-130a-3p arrests CNE-2Z cells at G0/G1 stage and promotes apoptosis

CNE-2Z cells transfected with miR-130a-3p mimics [(60.16±1.29)%] had a larger number at the G0/G1 stage than the NC [(55.39±1.07)%], whereas cells in the G2 or S stages were no significant discrepancy (**Figure 3A**). Besides, the miR-130a-3p mimics group had a significantly higher apoptosis rate than control and NC groups, which indicated that the overexpression of miR-130a-3p could promote apoptosis of CNE-2Z cells (**Figure 3B**).

MiR-130a-3p binding to 3'UTR region of CXCL12 and down-regulating CXCL12 expression

According to the prediction by TargetScan database (http://www.targetscan.org), C*XCL12* could be one of the target genes of miR-130a-3p (**Figure 4A**). In the dual-luciferase reporter assay, only the cells in the wt-3'UTR+miR-130a-3p mimics group had a remarkably lower luciferase activity than other groups, suggesting that miR-130a-3p could bind to 3'UTR of *CXCL12* to restrain translation (**Figure 4B**). RT-qPCR and Western Blot were performed to quantify *CXCL12* mRNA and protein levels, respectively. Consistent results were showed out that si-*CXCL12* could apparently restrain *CXCL12* expression in CNE-2Z cells, pcDNA3.1 *CXCL12* group successfully higher expressed *CXCL12* in CNE-2Z cells and miR-mimics prominently decreased *CXCL12* mRNAs and proteins expression (**Figure 4C**, **4D**).

MiR-130a-3p suppresses CNE-2Z cell migration, viability, proliferation and invasion by targeting CXCL12

Scratch-wound assay was performed to evaluate CNE-2Z cells migration function, the results manifest that *CXCL12* might have a meaning

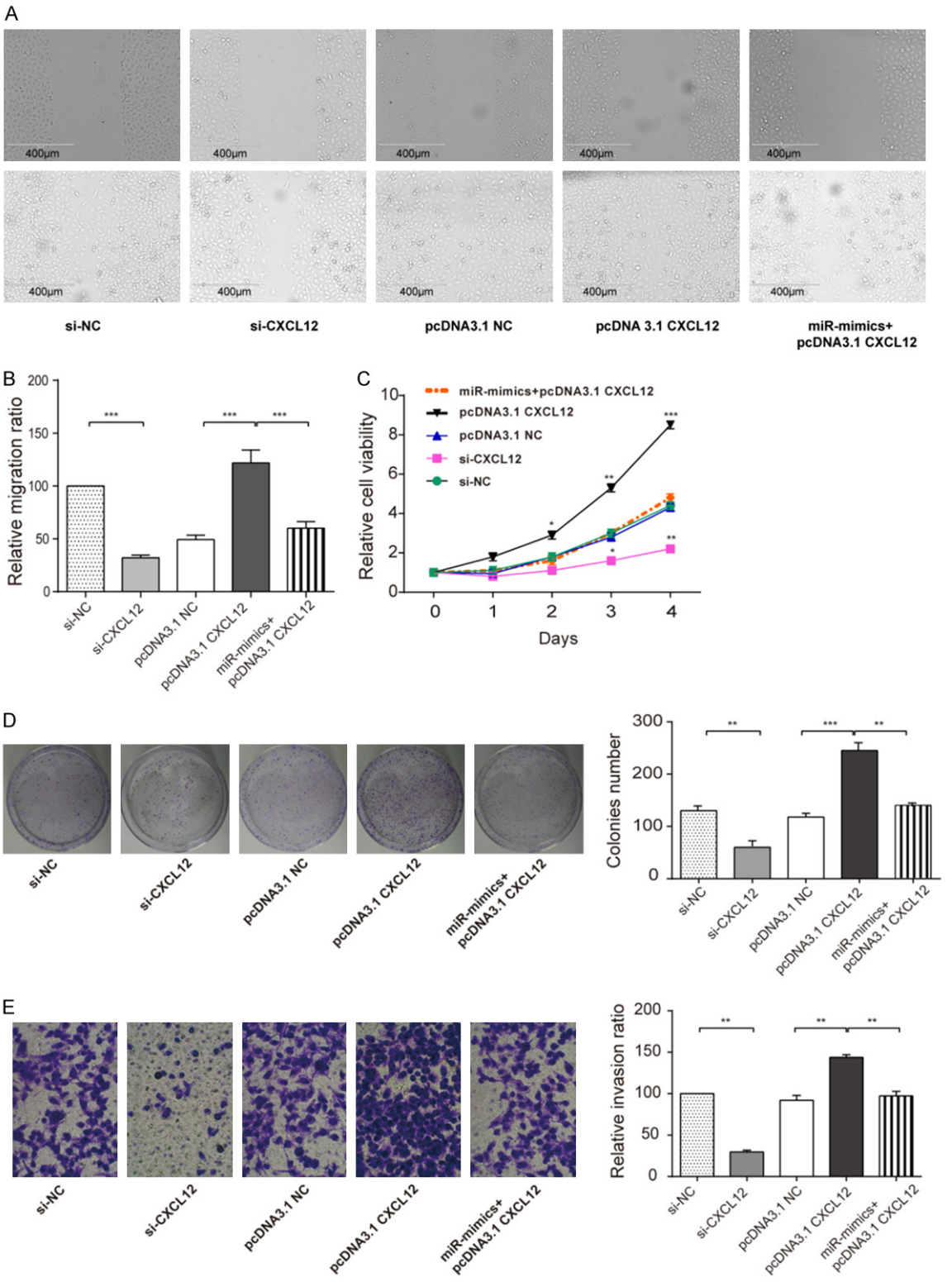

Figure 5. MiR-130a-3p target *CXCL12* resulted in suppressed CNE-2Z cell migration, viability, proliferation and invasion. (A) Scratch assay was done to analyze cell migration ability. (B) The cylindrical analysis diagram of relative migration ratio for picture A. (C) MTT assay was performed to analyze CNE-2Z cell viability at different time points (1-4 days), (D) Colony formation assay was also done to measure CNE-2Z cell proliferation rate. (E) Transwell assay was performed to analyze cell invasion ability, All the results showed a similar change that knockdown (si-*CXCL12*) the *CXCL12* had lower relative migration ratio, lower relative cell viability, lower colonies number, lower relative invasion ratio, whereas overexpression (pcDNA3.1-*CXCL12*) all in higher level. MiR-130a-3p decreased the over-expressed higher level (miR-mimics+pcDNA3.1-*CXCL12*). (student *t*-test **P*<0.05, ***P*<0.01, ****P*<0.001). Each assay was conducted in triplicate and repeated three times. The data show the mean of triplicaterepeats ± s.e.m.

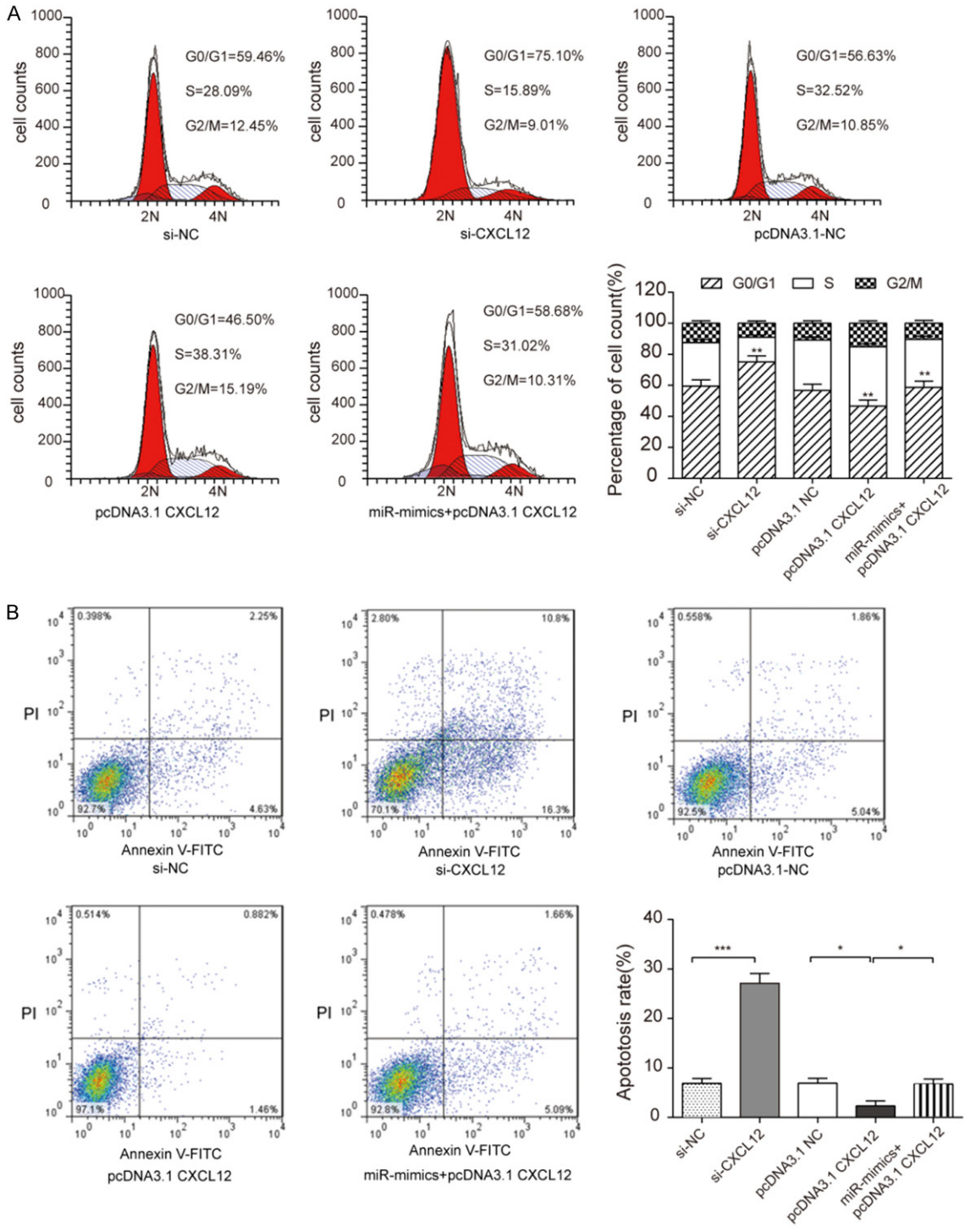

Figure 6. MiR-130a-3p inhibiting *CXCL12* affected CNE-2Z cell cycle and promoted cell apoptosis. A: Flow cytometry (PI staining) results showed that si-*CXCL12* group had the highest cells at G0/G1 stage, pcDNA3.1-*CXCL12* had the lowest and miR-mimics+pcDNA3.1-*CXCL12* had the middle cell count (student *t*-test, $^{**}P<0.01$). B: Annexin V and PI staining detected CNE-2Z cells apoptosis. Si-*CXCL12* group had the highest ratio, while pcDNA3.1-*CXCL12* had the lowest ratio. MiR-mimics+pcDNA3.1-*CXCL12* had a higher than pcDNA3.1-*CXCL12* but lower than si-*CXCL12* (student *t*-test, $^{*}P<0.05$, $^{***}P<0.001$). Each assay was conducted in triplicate and repeated three times. The data show the mean of triplicate repeats ± s.e.m.

effect on NE-2Z cells migration (i.e. si-*CXCL12*), overexpressed *CXCL12* could notably increase migratory ratio (i.e. pcDNA3.1 *CXCL12*) and miR-130a-3p mimics could prominently restrain this function (i.e. miR-mimics+pcDNA3.1 *CXCL12*) (**Figure 5A**, **5B**). MTT assay was performed to assess the viability of cells. Compared with NC group, the CNE-2Z cell OD value sharply dropped when *CXCL12* was knocked down (i.e. si-*CXCL12*). Compared with pcDNA3.1 NC, the proliferation of CNE-2Z significantly increased when *CXCL12* was over-expressed (i.e. pcDNA3.1 *CXCL12*) (**Figure 5C**). MiR-130a-3p mimics could prominently counteract this function likewise (i.e. miR-mimics+pcDNA3.1 *CXCL12*). The colony formation assay was performed to observe influence on CNE-2Z cell proliferation. The results showed that *CXCL12* had an effect on CNE-2Z cells proliferation (i.e. si-*CXCL12* and pcDNA3.1 *CXCL12*), overexpressed *CXCL12* could strengthen proliferation of CNE-2Z cells (i.e. pcDNA3.1 *CXCL12*) and miR-130a-3p mimics could restrain proliferation (i.e. miR-mimics+pcDNA3.1 *CXCL12*) (**Figure 5D**). Transwell assay was performed to assess the cell invasion rate (**Figure 5E**). The invasion rate of CNE-2Z cells markedly dropped when *CXCL12* was knocked down (i.e. si-*CXCL12*), which meant that the inhibition of *CXCL12* could suppress CNE-2Z cell invading. Compared with pcDNA3.1 *CXCL12* group (143.7±3.26%), CNE-2Z cells in miR-mimics+pcDNA3.1-*CXCL12* (97.27±5.45%) group showed the offsetting effect of invasion ability (97.3±4.2%), which demonstrated that miR-130a-3p could inhibit CNE-2Z cell invasion rate via down-regulating *CXCL12*.

MiR-130a-3p inhibiting CXCL12 to affect CNE-2Z cell cycle and apoptosis

The effects of *CXCL12* on cell cycle and apoptosis were measured by a flow cytometer (**Figure 6A**). The results testified to knockdown *CXCL12* (i.e. si-*CXCL12*) blocked cell cycle to stay G0/G1 stage, which cells could not effectively differentiated and proliferated, overexpressing *CXCL12* (i.e. pcDNA3.1-*CXCL12*) made more cells stay S stage. Similarly, miR-mimics+pcDNA3.1-*CXCL12* group compared to pcDNA3.1-*CXCL12* group had a higher proportion at G0/G1 [(56.83±4.14)%>(40.9±2.17)%] and a lower proportion at S stage [(32.07±3.51)%<(37.12±3.04)%]. si-*CXCL12* group had a higher apoptosis rate [(23.3±2.84)%] compared with NC group [(4.5±2.56)%]. Overexpress *CXCL12* (pcDNA3.1-*CXCL12*), the apoptosis rate would decrease [(1.2±2.9)%], nevertheless miR-mimics+pcDNA3.1-*CXCL12* group reversed this effect [(5.5±3.01)%] (**Figure 6B**).

Discussion

MiRNAs have been demonstrated to be dysregulated in NPC tissues based on previous studies. For instance, miR-34a-5p, miR-449a and miR-183 were reported to affect the proliferation, migration and invasion of NPC cells [20-23]. Consistent with our in vitro studies that proliferation, migration and invasion of NPC cells could be suppressed by over-expressed miR-130a-3p, which indicated that miR-130a-3p might play a role in the development and progression of NPC. MiR-130a-3p was firstly reported to participate in the activation of platelet physiology by targeting the transcription factor MAFB [24]. Later studies suggested that miR-130a-3p could affect a cluster of cancers, including hepatoma, triple-negative breast cancer and urinary bladder cancer [15, 25, 26]. In our study, miR-130a-3p was suggested as a NPC suppressor that could negatively influence proliferation and invasion of NPC cells.

CXCL12 was indicated to play an essential role in hematopoiesis in previous studies [27-29]. To be specific, Arabanian *et al.* suggested that *CXCL12* appeared to trigger the entry of more mature hematopoietic stem and progenitor cells into the cell cycle [30]. *CXCL12* could counteract cell apoptosis and recruit progenitor cells by combining with its receptor CXCR4 [31]. *CXCL12* also had a suppressing effect on papillary thyroid carcinoma and to be look as a powerful prognostic biomarker in prostate cancer [32, 33]. Studies also confirmed that CXCR4/CXCR7-*CXCL12* axis could exacerbate NPC cell migration and invasion [34], which is consistent with our study. The cancer facilitator role of *CXCL12* was further confirmed in the present study.

Oncogenes had been identified and confirmed to be targets of miR-130a-3p. For instance, Smad4 could be regulated by miR-130a-3p in gemcitabine-resistant hepatoma cells [15].

CXCL12 was predicted to be a potential target of miR-130a-3p by TargetScan, and this target relationship was confirmed by dual luciferase reporter gene assay. RT-qPCR and western blot, the abundance of *CXCL12* mRNA and protein in CNE-2Z cells was reduced after transfected with miR-130a-3p. Thus in this study, we validated the cancer suppressor role of miR-130a-3p by possibly binding to the oncogene *CXCL12* mRNA.

The limitation of our study was that the complicated regulatory network of *CXCL12* and miRNAs were not entirely investigated. Various factors involved in the regulation of *CXCL12*, and miR-130a-3p also had multiple targets other than *CXCL12* such as oncogene MDM4, but our study merely contributed to mapping one part of the whole regulatory network in NPC pathogenesis. Besides, both miR-130a-3p and *CXCL12* had been proved to have close correlations with hematopoiesis [27-29], but whether the hematopoietic function participated in the NPC progression remained vague to us. Thus it would be deserved to study if hematopoiesis took part in the process of NPC inhibition in further.

In conclusion, our study further confirmed the role of *CXCL12* and miR-130a-3p in modifying NPC cells. The targeting relationship between them provided novel insights into the mechanisms of the caner suppressive features of miR-130a-3p in NPC, indicating that miR-130a-3p and *CXCL12* might serve as potential therapeutic targets for NPC.

Disclosure of conflict of interest

None.

Abbreviations

NPC, Nasopharyngeal carcinoma; miRNAs, MicroRNAs; 3'UTR, 3'-untranslated region; *CXCL12*, C-X-C motif chemokine ligand 12; NC, negative control.

Address correspondence to: Dongrui Guo, Department of Hematology and Oncology, The Second Hospital of Jilin University, No. 218 Ziqiang Street, Nanguan District, Changchun 130041, Jilin, China. Tel: +86 0431 88796827; E-mail: zhengyuling666@163.com

References

[1] Jemal A, Bray F, Center MM, Ferlay J, Ward E and Forman D. Global cancer statistics. CA Cancer J Clin 2011; 61: 69-90.

[2] Lai SZ, Li WF, Chen L, Luo W, Chen YY, Liu LZ, Sun Y, Lin AH, Liu MZ and Ma J. How does intensity-modulated radiotherapy versus conventional two-dimensional radiotherapy influence the treatment results in nasopharyngeal carcinoma patients? Int J Radiat Oncol Biol Phys 2011; 80: 661-668.

[3] Colaco RJ, Betts G, Donne A, Swindell R, Yap BK, Sykes AJ, Slevin NJ, Homer JJ and Lee LW. Nasopharyngeal carcinoma: a retrospective review of demographics, treatment and patient outcome in a single centre. Clin Oncol (R Coll Radiol) 2013; 25: 171-177.

[4] Jia WH, Huang QH, Liao J, Ye W, Shugart YY, Liu Q, Chen LZ, Li YH, Lin X, Wen FL, Adami HO, Zeng Y and Zeng YX. Trends in incidence and mortality of nasopharyngeal carcinoma over a 20-25 year period (1978/1983-2002) in Sihui and Cangwu counties in southern China. BMC Cancer 2006; 6: 178.

[5] He L and Hannon GJ. MicroRNAs: small RNAs with a big role in gene regulation. Nat Rev Genet 2004; 5: 522-531.

[6] Calin GA and Croce CM. MicroRNA signatures in human cancers. Nat Rev Cancer 2006; 6: 857-866.

[7] Lu J, Getz G, Miska EA, Alvarez-Saavedra E, Lamb J, Peck D, Sweet-Cordero A, Ebert BL, Mak RH, Ferrando AA, Downing JR, Jacks T, Horvitz HR and Golub TR. MicroRNA expression profiles classify human cancers. Nature 2005; 435: 834-838.

[8] Volinia S, Calin GA, Liu CG, Ambs S, Cimmino A, Petrocca F, Visone R, Iorio M, Roldo C, Ferracin M, Prueitt RL, Yanaihara N, Lanza G, Scarpa A, Vecchione A, Negrini M, Harris CC and Croce CM. A microRNA expression signature of human solid tumors defines cancer gene targets. Proc Natl Acad Sci U S A 2006; 103: 2257-2261.

[9] Xiao J, Li Y, Zhang W, Jiang Y, Du B and Tan Y. miR-34b inhibits nasopharyngeal carcinoma cell proliferation by targeting ubiquitin-specific peptidase 22. Onco Targets Ther 2016; 9: 1525-1534.

[10] Tian Y, Cai L, Tian Y, Tu Y, Qiu H, Xie G, Huang D, Zheng R and Zhang W. miR156a mimic represses the epithelial-mesenchymal transition of human nasopharyngeal cancer cells by targeting junctional adhesion molecule A. PLoS One 2016; 11: e0157686.

[11] Zhang Z, Ma J, Luan G, Kang L, Su Y, He Y and Luan F. MiR-506 suppresses tumor prolifera-

tion and invasion by targeting FOXQ1 in nasopharyngeal carcinoma. PLoS One 2015; 10: e0122851.
[12] Zhang X, Huang L, Zhao Y and Tan W. Downregulation of miR-130a contributes to cisplatin resistance in ovarian cancer cells by targeting X-linked inhibitor of apoptosis (XIAP) directly. Acta Biochim Biophys Sin (Shanghai) 2013; 45: 995-1001.
[13] Zhou YM, Liu J and Sun W. MiR-130a overcomes gefitinib resistance by targeting met in non-small cell lung cancer cell lines. Asian Pac J Cancer Prev 2014; 15: 1391-1396.
[14] Fujita Y, Kojima T, Kawakami K, Mizutani K, Kato T, Deguchi T and Ito M. miR-130a activates apoptotic signaling through activation of caspase-8 in taxane-resistant prostate cancer cells. Prostate 2015; 75: 1568-1578.
[15] Liu Y, Li Y, Wang R, Qin S, Liu J, Su F, Yang Y, Zhao F, Wang Z and Wu Q. MiR-130a-3p regulates cell migration and invasion via inhibition of Smad4 in gemcitabine resistant hepatoma cells. J Exp Clin Cancer Res 2016; 35: 19.
[16] Secchiero P, Celeghini C, Cutroneo G, Di Baldassarre A, Rana R and Zauli G. Differential effects of stromal derived factor-1 alpha (SDF-1 alpha) on early and late stages of human megakaryocytic development. Anat Rec 2000; 260: 141-147.
[17] Kinose Y, Sawada K, Nakamura K and Kimura T. The role of microRNAs in ovarian cancer. Biomed Res Int 2014; 2014: 249393.
[18] Zhao YN, Chen GS and Hong SJ. Circulating MicroRNAs in gynecological malignancies: from detection to prediction. Exp Hematol Oncol 2014; 3: 14.
[19] Nagasawa T. CXCL12/SDF-1 and CXCR4. Front Immunol 2015; 6: 301.
[20] Wang F, Lu J, Peng X, Wang J, Liu X, Chen X, Jiang Y, Li X and Zhang B. Integrated analysis of microRNA regulatory network in nasopharyngeal carcinoma with deep sequencing. J Exp Clin Cancer Res 2016; 35: 17.
[21] Song P, Ye LF, Zhang C, Peng T and Zhou XH. Long non-coding RNA XIST exerts oncogenic functions in human nasopharyngeal carcinoma by targeting miR-34a-5p. Gene 2016; 592: 8-14.
[22] Li H, Li X, Ge X, Jia L, Zhang Z, Fang R, Yang J, Liu J, Peng S, Zhou M, Xiang J, Zeng Z, Zhou W, Xiong W, Xiao G, Fang L, Li GY and Li Z. MiR-34b-3 and miR-449a inhibit malignant progression of nasopharyngeal carcinoma by targeting lactate dehydrogenase A. Oncotarget 2016; 7: 54838-54851.
[23] Cheung CC, Lun SW, Chung GT, Chow C, Lo C, Choy KW and Lo KW. MicroRNA-183 suppresses cancer stem-like cell properties in EBV-associated nasopharyngeal carcinoma. BMC Cancer 2016; 16: 495.
[24] Garzon R, Pichiorri F, Palumbo T, Iuliano R, Cimmino A, Aqeilan R, Volinia S, Bhatt D, Alder H, Marcucci G, Calin GA, Liu CG, Bloomfield CD, Andreeff M and Croce CM. MicroRNA fingerprints during human megakaryocytopoiesis. Proc Natl Acad Sci U S A 2006; 103: 5078-5083.
[25] Ouyang M, Li Y, Ye S, Ma J, Lu L, Lv W, Chang G, Li X, Li Q, Wang S and Wang W. MicroRNA profiling implies new markers of chemoresistance of triple-negative breast cancer. PLoS One 2014; 9: e96228.
[26] Segersten U, Spector Y, Goren Y, Tabak S and Malmstrom PU. The role of microRNA profiling in prognosticating progression in Ta and T1 urinary bladder cancer. Urol Oncol 2014; 32: 613-618.
[27] Itkin T, Gur-Cohen S, Spencer JA, Schajnovitz A, Ramasamy SK, Kusumbe AP, Ledergor G, Jung Y, Milo I, Poulos MG, Kalinkovich A, Ludin A, Kollet O, Shakhar G, Butler JM, Rafii S, Adams RH, Scadden DT, Lin CP and Lapidot T. Distinct bone marrow blood vessels differentially regulate haematopoiesis. Nature 2016; 532: 323-328.
[28] Voermans C, van Hennik PB and van der Schoot CE. Homing of human hematopoietic stem and progenitor cells: new insights, new challenges? J Hematother Stem Cell Res 2001; 10: 725-738.
[29] Mendt M and Cardier JE. Role of SDF-1 (CXCL12) in regulating hematopoietic stem and progenitor cells traffic into the liver during extramedullary hematopoiesis induced by G-CSF, AMD3100 and PHZ. Cytokine 2015; 76: 214-221.
[30] Arabanian LS, Fierro FA, Stolzel F, Heder C, Poitz DM, Strasser RH, Wobus M, Borhauser M, Ferrer RA, Platzbecker U, Schieker M, Docheva D, Ehninger G and Illmer T. MicroRNA-23a mediates post-transcriptional regulation of CXCL12 in bone marrow stromal cells. Haematologica 2014; 99: 997-1005.
[31] Zernecke A, Bidzhekov K, Noels H, Shagdarsuren E, Gan L, Denecke B, Hristov M, Koppel T, Jahantigh MN, Lutgens E, Wang S, Olson EN, Schober A and Weber C. Delivery of microRNA-126 by apoptotic bodies induces CXCL12-dependent vascular protection. Sci Signal 2009; 2: ra81.
[32] Dong S, Jin M, Li Y, Ren P and Liu J. MiR-137 acts as a tumor suppressor in papillary thyroid carcinoma by targeting CXCL12. Oncol Rep 2016; 35: 2151-2158.

[33] Goltz D, Holmes EE, Gevensleben H, Sailer V, Dietrich J, Jung M, Rohler M, Meller S, Ellinger J, Kristiansen G and Dietrich D. CXCL12 promoter methylation and PD-L1 expression as prognostic biomarkers in prostate cancer patients. Oncotarget 2016; 7: 53309-53320.

[34] Qiao N, Wang L, Wang T and Li H. Inflammatory CXCL12-CXCR4/CXCR7 axis mediates G-protein signaling pathway to influence the invasion and migration of nasopharyngeal carcinoma cells. Tumour Biol 2016; 37: 8169-8179.